



Detecting gravitational waves via coherence degradation induced by the Unruh effect

Pedro H. M. Barros^a , Helder A. S. Costa^b 

Departamento de Física, Universidade Federal do Piauí, Ininga, Teresina, Piauí 64049-550, Brazil

Received: 5 July 2024 / Accepted: 21 November 2024
© The Author(s) 2024

Abstract We investigate the effects of a gravitational wave background on the coherence degradation induced by the Unruh effect of a uniformly accelerated single-qubit and quantum interferometric circuit. In both systems, we use the formalism of the evolution of the density matrix of the detector-field system, where after the interaction the field degrees of freedom are traced out to obtain the reduced density matrix of the detector. In this background, we calculate the quantum coherence and interferometric visibility in the long-wavelength regime and large interaction time. Our results indicate that the gravitational wave transfers energy to the internal states of the detector, causing, together with the Unruh effect, changes in them, amplifying the coherence degradation of the system. This amplification occurs when the polarization modes of the gravitational wave are in resonance and have modulated amplitudes. For the case of a short-wavelength, the detector does not respond to the gravitational wave because its oscillation is so fast that the detector does not have time to respond within the system timescale. Therefore, it is possible to detect the signature of gravitational waves in the coherence degradation induced by the Unruh effect within the regimes studied here.

1 Introduction

It is well known that quantum mechanics and relativity are the two pillars that support the foundations of modern physics. On the other hand, although these two theories are the most beautiful and powerful theories we have about the universe, they are not completely compatible with each other. Many efforts were made to reduce the incompatibility gap between these theories, and thus quantum field theory (QFT) was born,

it treats particles as excited states of their underlying quantum fields. A very interesting prediction of this theory is the well-known Fulling–Davies–Unruh effect [1–3], or simply Unruh effect, which predicts that a non-inertial observer in accelerated motion will see the Minkowski vacuum state as a thermal bath of excited particles. Moreover, the notion of particles is quite ambiguous for QFT in curved spacetime due to the occurrence of the number of particles is not well defined, therefore, an definition in terms of the response of a “particle detector” is necessary. In 1976, Unruh proposed a theoretical model of a particle detector [3] idealized as a point object in a box that interacts with a quantum field, thus, it is said that a particle in this field is detected if the object in the box is excited from its initial ground state to some excited state. In 1979, DeWitt [4] improved the idea simplifying the Unruh model as a two-level monopole detector, which became widely known as the Unruh–DeWitt detector, it is currently widely used in various physics contexts.

In recent years, relativistic quantum information (RQI) has emerged, a new field of research consisting of the concepts of gravitational physics and quantum computing, which aims to understand the role of relativity in quantum information processing protocols [5]. Even disregarding attempts at quantum gravity, we will still have a huge list of investigations into RQI that are distinct from each other, such as: the use of quantum probes to investigate the Unruh and Hawking effect [3, 4, 6, 7] and the construction of relativistic protocols [8–15] as this paper also addresses.

Furthermore, we can indirectly measure the creation of particles due to the Unruh effect through quantum coherence, which provides the ability of a system to maintain the superposition of its states [16], so when these states are subjected to the Unruh effect the presence of created particles accelerate the degradation of coherence, as well shown in some studies [17–25]. The quantum fluctuations of the background field act as an environment, according to [26], then it is important

^a e-mail: phmbarros@ufpi.edu.br (corresponding author)

^b e-mail: hascosta@ufpi.edu.br

to emphasize that the loss of coherence (or coherence degradation if you prefer) can be amplified as long as we manage to intensify the Unruh effect. There are many ways to achieve this, such as transferring energy to the quantum fluctuations of the background field, which consequently increase the effects of the environment. Using quantum interferometry [24, 27–29], we can indirectly measure the properties of a system to extract information about a specific component of this system through a probe. Quantum scattering circuits have several applications such as: testing the Leggett–Garg inequality [30], simulating Fano–Anderson problems [31], discrete Wigner functions [32], and many other examples.

Primitive studies [33–40] investigated how planar gravitational waves influence scalar fields, in this way, recent studies [41, 42] has shown how an Unruh–DeWitt detector responds to the gravitational wave background, the findings of these works showed that the response of the detector is different from the result without a gravitational wave, obeying the conditions established for each case. In reference [41], the response of the detector in the gravitational wave background was studied in the long-wavelength and short-wavelength regimes, the authors found that in the case of a trajectory in constant acceleration in the long-wavelength regime, the detector’s response is modified. On the other hand, for a detector following the same trajectory in the short-wavelength regime, the detector does not reply. Additionally, a very robust study involving gravitational waves in Rindler spaces was carried out in [43], which derives the gravitational wave solutions in the left and right Rindler wedges analytically.

Therefore, in this work we investigate how a gravitational wave background can influence the coherence degradation mechanism induced by the Unruh effect of an accelerated single-qubit and quantum interferometric circuit. In this investigation we use two setups: The first is composed of a uniformly accelerated detector that is prepared in an initial superposition state of a qubit, then interacts with a massless scalar field and finally has its internal states measured. In this investigation we use two setups: The first is composed of a two-level system initially prepared in a qubit state that is uniformly accelerated and interacts with a massless scalar field for a finite time. The second is a quantum interferometric circuit composed of a Hadamard gate, a phase change gate together with the detector-field interaction, another Hadamard gate and, finally, measurement of the internal states of the detector.

This article is structured as follows: In Sect. 2, we describe the physical model of an Unruh–DeWitt detector in the gravitational wave background, calculate the transition probability rates for the short- and long-wavelength regimes. Subsequently, we study in Sect. 3, the influence of the gravitational wave background on the loss of coherence of an accelerated single-qubit, here we calculate the l^1 norm quantum

coherence. In Sect. 4, we study the quantum interferometric circuit, where through maximum and minimum probability we obtain interferometric visibility in a gravitational wave background. We perform an analysis in Sect. 5 of the numerical results of the accelerated single-qubit coherence and the visibility of the quantum interferometric circuit to visualize the new physical effects. Finally, in the last section, we present the conclusions of our paper. In Appendix, we briefly reviewed the model that describes the Klein–Gordon equation and its quantization in the gravitational wave background.

The entire content of this work uses the system of natural units, in which the speed of light and the Planck constant are written as the unit ($c = \hbar = 1$).

2 The Unruh–DeWitt detector

To obtain the response of an Unruh–DeWitt detector during a finite interaction time, we consider a model that has two energy levels, $|g\rangle$ and $|e\rangle$, coupled to a real, free, massless scalar field ϕ , through a monopole interaction. Considering that the detector travels along a world line $x(\tau)$, and the field is in the vacuum state $|0\rangle$, where τ is the detector’s own time, the Hamiltonian for the monopole interaction is given by

$$\mathcal{H}_{\text{int}} = \lambda \Theta(\tau) \mu(\tau) \phi[x(\tau)], \quad (1)$$

where λ is a small coupling constant, $\Theta(\tau)$ is the switching function which accounts for the switch-on and switch-off of the detector, and $\mu(\tau)$ is the operator of the detector’s monopole moment. $\Theta(\tau)$ is considered a window function and has the properties: $\Theta(\tau) \approx 1$ for $|\tau| \ll T$ and $\Theta(\tau) \approx 0$ for $|\tau| \gg T$, where T is the interaction time. For these conditions, considering up to the first order of interaction, we have that the probabilities of excitation (absorption) and de-excitation (emission) are, respectively, written as $P^\pm = \lambda^2 |\langle g | \mu(0) | e \rangle|^2 \mathcal{F}^\pm$, where \mathcal{F}^\pm are known as response functions, given by

$$\mathcal{F}^\pm = \int_{-\infty}^{\infty} d\tau \int_{-\infty}^{\infty} d\tau' \Theta(\tau) \Theta(\tau') e^{\pm i\Omega(\tau - \tau')} G^\pm[x(\tau), x(\tau')] \quad (2)$$

where Ω is the transition angular frequency, with: excitation ($\Omega > 0$) and de-excitation ($\Omega < 0$). And the well-known Wightman function given by

$$G^+[x(\tau), x(\tau')] = \langle 0_{\mathcal{M}} | \phi[x(\tau)] \phi[x(\tau')] | 0_{\mathcal{M}} \rangle \quad (3)$$

where along inertial and accelerated trajectories, Eq. (3) is invariant under temporal translation, this in Minkowski space and in the detector frame, and for this case we have $G^+[x(\tau), x(\tau')] = G^+(\tau - \tau')$ [44, 45]. Using the Gaussian

window function $\Theta(\tau) = \exp\left(-\frac{\tau^2}{2T^2}\right)$, we obtain transition probability per unit time (with finite interaction time) is given by [46]

$$R^\pm \approx R^\pm(\infty) + \frac{1}{2T^2} \frac{\partial^2 R^\pm(\infty)}{\partial \Omega^2} + \mathcal{O}\left(\frac{1}{T^4}\right), \tag{4}$$

where R^- and R^+ being the rates of the excitation probability and the de-excitation probability, respectively.

Now, we need to find a closed expression for the response function (2) in a monochrome gravitational wave background, and note that to do this we will first have to obtain the Wightman function for the mode expansion obtained at the end of the Appendix. Thus, using the mode expansion (48) in the expression of the Wightman function (3), as shown in [41], we have

$$G^+(x, x') = \int \frac{d^3k}{(2\pi)^3} \frac{1}{2k_\mu} e^{i\mathbf{k}\cdot(\mathbf{x}-\mathbf{x}')} e^{-ik_\mu(u-u')} e^{-i\omega_{\mathbf{k},\mathbf{k}}(v-v')} \times e^{ik_{u,c}(\mathbf{k})(\sin \omega' u - \sin \omega' u')/\omega'} e^{ik_{u,s}(\mathbf{k})(\cos \omega' u - \cos \omega' u')/\omega'}. \tag{5}$$

As we can see this expression does not have a closed form, it is possible to simplify it if we consider the long-wavelength condition and the short-wavelength condition. Naturally, the Unruh–DeWitt detector gives two time scales: The first is the response time for the transition of a two-level system, $\approx 1/\Omega$. The second characterizes the detector activation period, $\approx T$. In fact, a detector is always on for only a finite period T , which establishes a time scale to be compared with the period $1/\omega$ of the gravitational wave. Thus, the transition rate resulting from the Unruh–DeWitt detector is legitimate only if the measurement performed at time τ is within the activation period. Consequently, the condition $1 \ll \Omega T$ must be satisfied to produce a sensible result. The gravitational wave background is at the extreme end of the long-wavelength spectrum. When the wavelength of these gravitational waves is so long that, throughout the detector’s operating period, no modulation in the wave is observed, but only a persistent amplitude of the gravitational wave is perceived.

Therefore, considering a gravitational plane wave propagating in the z direction, ($k = \omega > 0$), the condition for the long wavelength condition written as $1/\Omega \ll T \ll \sqrt{1 - v^2}/|v_z - 1|\omega$, where \mathbf{v} is the detector’s moving velocity (averaged over the switch-on period). Not considering corrections equal to or greater than the order of $\mathcal{O}(\omega T)$, we can take the formal limit $\omega \rightarrow 0$ for the long-wavelength limit result. In this formal condition, the phase of the gravitational wave must be treated as the same as in the hypersurface $u = 0$. Thus, the persistent amplitude detected during T is given by $h_{+/\times}(x)|_{u=0} \equiv A_{+/\times} \cos \delta_{+/\times}$, for the plus (+) and cross (\times) modes, respectively. Thus, for a system in which the long-wavelength condition is satisfied, then we can consider $\mathcal{A}_{+/\times} = A_{+/\times} \cos \delta_{+/\times}$ (in the formal limit) can

represent the persistent amplitudes detected during the finite time T . Therefore, using this information, we can obtain the Wightman function in a monochromatic gravitational wave background for long-wavelength condition, given by

$$G_{\text{Iw}}^+(x - x') = -\frac{1}{8\pi} \frac{1}{\sqrt{1 - \mathcal{A}^2}} \frac{1}{(u - u' - i\epsilon)(v - v' - i\epsilon) - D(\Delta x, \Delta y)/2}, \tag{6}$$

where $D(\Delta x, \Delta y) = [(1 + \mathcal{A}_+) \Delta x^2 + 2\mathcal{A}_\times \Delta x \Delta y + (1 - \mathcal{A}_+) \Delta y^2]/(1 - \mathcal{A}^2)$, with $\mathcal{A}^2 = \mathcal{A}_+^2 + \mathcal{A}_\times^2$.

For the short-wavelength condition, we have $\sqrt{1 - v^2}/|v_z - 1|\omega \ll 1/\Omega \ll T$ indicating that the detected gravitational wave modulation frequency is much higher than the two-level transition angular frequency Ω . Not considering any corrections equal to or greater than the order of $\mathcal{O}(\Omega/\omega)$, we can simply take the formal limit $\omega \rightarrow \infty$ for the short-wavelength limit result. For this condition, we observe that the Wightman function does not depend on the amplitudes of the gravitational wave, and this implies

$$G_{\text{sw}}^+(x - x') = G_{\text{M}}^+(x - x'), \tag{7}$$

and so we can see that the Wightman function in a gravitational wave background in the short-wavelength condition is exactly the same as that given in Minkowski space.

Given the results obtained, we can study the response of an Unruh–DeWitt detector along a trajectory with constant acceleration a in the z direction, and then

$$t = \frac{1}{a} \sinh a\tau, \quad z = \frac{1}{a} \cosh a\tau, \quad x = y = 0. \tag{8}$$

Replacing (8) in (6) and in (7), we then have $G_{\text{sw}}^+(x - x') = G_{\text{M}}^+(x - x')$ and

$$G_{\text{Iw}}^+(\Delta\tau) = \frac{-1}{4\pi^2} \frac{1}{\sqrt{1 - \mathcal{A}^2}} \sum_{k=-\infty}^{\infty} \frac{1}{(\Delta\tau - i\epsilon + 2\pi ik/a)^2}. \tag{9}$$

Note that, for the short-wavelength condition, we saw that the Wightman function is the same as that given by Minkowski space, and because of this we are guaranteed that the transition probabilities and probability transition rates are the same given in Minkowski space. Now, for the long-wavelength condition, the Wightman function has a dependence on the amplitudes and phase shifts of the gravitational wave, thus, replacing (9) in (4), we obtain

$$\overline{R}_{\text{Iw}}^- \approx \frac{1}{2\pi} \frac{1}{\sqrt{1 - \mathcal{A}^2}} \frac{1}{e^{2\pi/\bar{a}} - 1} \left\{ 1 + \frac{2\pi}{\bar{a}\sigma^2} \frac{e^{2\pi/\bar{a}}}{e^{2\pi/\bar{a}} - 1} \left[1 - e^{2\pi/\bar{a}} + \frac{\pi}{\bar{a}} \left(e^{2\pi/\bar{a}} + 1 \right) \right] \right\}, \tag{10}$$

$$\overline{R}_{\text{Iw}}^+ \approx \frac{1}{2\pi} \frac{1}{\sqrt{1-\mathcal{A}^2}} \frac{e^{2\pi/\bar{a}}}{e^{2\pi/\bar{a}}-1} \left\{ 1 + \frac{2\pi}{\bar{a}\sigma^2} \frac{1}{e^{2\pi/\bar{a}}-1} \left[1 - e^{2\pi/\bar{a}} + \frac{\pi}{\bar{a}} \left(e^{2\pi/\bar{a}} + 1 \right) \right] \right\}, \tag{11}$$

where $\overline{R}_{\text{Iw}}^- = R_{\text{Iw}}^-/\Omega$ is dimensionless, which are the probability rates of excitation R_{Iw}^- and de-excitation R_{Iw}^+ per unit of Ω in a gravitational wave background, where $\bar{a} = a/\Omega$ and $\sigma = \Omega T$ are dimensionless parameters. Note that when $\mathcal{A}_+ = \mathcal{A}_\times = 0$, we have that $\overline{R}_{\text{Iw}}^\pm = \overline{R}_{\text{M}}^\pm$, returning to the well-known standard case.

3 Accelerated single-qubit coherence degradation

Here in this section, we quantify the loss of coherence of a accelerated single-qubit due to the Unruh effect in a gravitational wave background, additionally, we obtain the coherence in order to investigate which effects arise in our system due to in a gravitational wave background. To achieve this, we constructed a schematic representation (as shown in Fig. 1) of our setup that illustrates the loss of coherence due to the Unruh effect of an accelerated detector. In our system we have a detector and a real, free, massless scalar field. The field is in a vacuum state presented in (51) in a spacetime that has a metric with a gravitational plane wave (42), while the detector is in a qubit state $|\psi_D\rangle = \alpha|g\rangle + \beta|e\rangle$, where $|\alpha|^2 + |\beta|^2 = 1$, or even in the representation of a vector on the Bloch sphere, it can be written as

$$|\psi_D\rangle = \cos \frac{\theta}{2} e^{i\chi/2} |g\rangle + \sin \frac{\theta}{2} e^{-i\chi/2} |e\rangle, \tag{12}$$

where $\alpha = \cos \frac{\theta}{2} e^{i\frac{\chi}{2}}$ and $\beta = \sin \frac{\theta}{2} e^{-i\frac{\chi}{2}}$. We can obtain the corresponding density matrix, given by the expression $\hat{\rho}_D^{\text{in}} = |\psi_D\rangle\langle\psi_D|$, and this expression results in

$$\hat{\rho}_D^{\text{in}} = |\alpha|^2 |g\rangle\langle g| + \alpha\beta^* |g\rangle\langle e| + \alpha^* \beta |e\rangle\langle g| + |\beta|^2 |e\rangle\langle e|, \tag{13}$$

where, in the context of the Bloch sphere, we have: $\theta \in [0, \pi]$ and $\chi \in [0, 2\pi]$ are the polar and azimuthal angles, respectively. After the detector is prepared in a qubit state, it interacts with the scalar field for a finite period T and then its internal states are measured.

Having knowledge of how the detector was initially prepared, we will now understand how the detector in a qubit state interacts with the scalar field in a gravitational wave background, this interaction is described by the expression given by $\hat{\rho}_{\text{in}} = \hat{\rho}_D^{\text{in}} \otimes \hat{\rho}_\phi$, where $\hat{\rho}_\phi = |0\rangle\langle 0|$, with the vacuum state in a gravitational wave background $|0\rangle$ being the one defined in (51). Considering the Hamiltonian described in (1) for a weak coupling, the resulting density matrix after

the interaction is written as

$$\hat{\rho}_{\text{out}} = \hat{U}^{(0)} \hat{\rho}_{\text{in}} \hat{U}^{(0)\dagger} + \hat{U}^{(1)} \hat{\rho}_{\text{in}} + \hat{\rho}_{\text{in}} \hat{U}^{(0)\dagger} + \hat{U}^{(1)} \hat{\rho}_{\text{in}} \hat{U}^{(1)\dagger} + \hat{U}^{(2)} \hat{\rho}_{\text{in}} \hat{U}^{(2)\dagger} + \mathcal{O}(g^3), \tag{14}$$

and here we have the well-known Temporal Evolution Operator, given by in a perturbative way

$$\hat{U} = \hat{U}^{(0)} + \hat{U}^{(1)} + \hat{U}^{(2)} + \mathcal{O}(g^3) \tag{15}$$

where

$$\hat{U}^{(0)} = \mathbb{I}, \tag{16}$$

$$\hat{U}^{(1)} = -i\lambda \int_{-\infty}^{\infty} d\tau \Theta(\tau) \mu(\tau) \phi[x(\tau)], \tag{17}$$

$$\hat{U}^{(2)} = -\lambda^2 \int_{-\infty}^{+\infty} d\tau \int_{-\infty}^{+\tau} d\tau' \Theta(\tau) \Theta(\tau') \mu(\tau) \mu(\tau') \phi[x(\tau)] \phi[x(\tau')], \tag{18}$$

with $\mu(\tau) = [\hat{\sigma}_+ e^{i\Omega\tau} + \hat{\sigma}_- e^{-i\Omega\tau}]$, being $\hat{\sigma}_+ = |e\rangle\langle g|$ and $\hat{\sigma}_- = |g\rangle\langle e|$ the raising and lowering operators, respectively. If we want to observe the state of the detector, we must exclude the consideration of the field, and because of this something different appears: the detector is in the ground or excited state, that is, this resulting state is no longer pure according to its initial form. The final result is obtained by the reduced density matrix, written as $\hat{\rho}_D^{\text{out}} = \text{Tr}_{|0\rangle}[\hat{\rho}_{\text{out}}]$, and from here on, we omit the superscript ‘‘out’’ for simplicity, in this way, tracing out the degrees of freedom of the field the reduced density matrix for the detector is given by the following expression

$$\hat{\rho}_{D,\text{Iw}} = \begin{pmatrix} \hat{\rho}_{D,\text{Iw}}^{\text{gg}} & \hat{\rho}_{D,\text{Iw}}^{\text{ge}} \\ \hat{\rho}_{D,\text{Iw}}^{\text{eg}} & \hat{\rho}_{D,\text{Iw}}^{\text{ee}} \end{pmatrix} \tag{19}$$

where

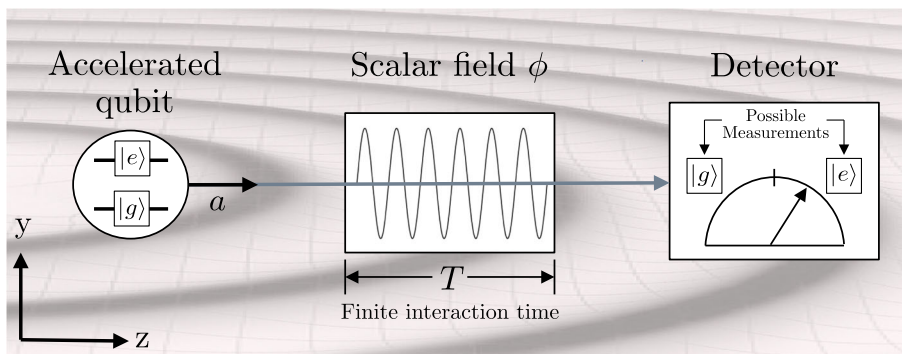
$$\hat{\rho}_{D,\text{Iw}}^{\text{gg}} = \cos^2 \frac{\theta}{2} + \lambda^2 \left[\sin^2 \frac{\theta}{2} \mathcal{F}_{\text{Iw}}^- - 2 \cos^2 \frac{\theta}{2} \text{Re}(\mathcal{G}_{\text{Iw}}^-) \right], \tag{20}$$

$$\hat{\rho}_{D,\text{Iw}}^{\text{ee}} = \sin^2 \frac{\theta}{2} + \lambda^2 \left[\cos^2 \frac{\theta}{2} \mathcal{F}_{\text{Iw}}^+ - 2 \sin^2 \frac{\theta}{2} \text{Re}(\mathcal{G}_{\text{Iw}}^+) \right], \tag{21}$$

$$\hat{\rho}_{D,\text{Iw}}^{\text{eg}} = \cos \frac{\theta}{2} \sin \frac{\theta}{2} e^{-i\chi} + \lambda^2 \left\{ \cos \frac{\theta}{2} \sin \frac{\theta}{2} \left[e^{i\chi} \mathcal{C}_{\text{Iw}}^+ - e^{-i\chi} (\mathcal{G}_{\text{Iw}}^+ + \mathcal{G}_{\text{Iw}}^{+*}) \right] \right\}, \tag{22}$$

$$\hat{\rho}_{D,\text{Iw}}^{\text{ge}} = \cos \frac{\theta}{2} \sin \frac{\theta}{2} e^{i\chi} + \lambda^2 \left\{ \cos \frac{\theta}{2} \sin \frac{\theta}{2} \left[e^{-i\chi} \mathcal{C}_{\text{Iw}}^- - e^{i\chi} (\mathcal{G}_{\text{Iw}}^- + \mathcal{G}_{\text{Iw}}^{-*}) \right] \right\}, \tag{23}$$

Fig. 1 Schematic representation of a qubit that is uniformly accelerated, interacts (for a time T) with a massless scalar field ϕ in a gravitational wave background. After the interaction, the qubit has its internal states measured by a detector



where

$$C_{lw}^{\pm} = \int_{-\infty}^{+\infty} d\tau \int_{-\infty}^{+\infty} d\tau' \Theta(\tau)\Theta(\tau') e^{\pm i\Omega(\tau+\tau')} G_{lw}(\tau, \tau'), \tag{24}$$

$$G_{lw}^{\pm} = \int_{-\infty}^{+\infty} d\tau \int_{-\infty}^{+\tau} d\tau' \Theta(\tau)\Theta(\tau') e^{\pm i\Omega(\tau-\tau')} G_{lw}(\tau, \tau'), \tag{25}$$

$$F_{lw}^{\pm} = \int_{-\infty}^{+\infty} d\tau \int_{-\infty}^{+\infty} d\tau' \Theta(\tau)\Theta(\tau') e^{\pm i\Omega(\tau-\tau')} G_{lw}(\tau, \tau'), \tag{26}$$

and

$$\text{Re}(G_{lw}^{\pm}) = \frac{1}{2} \left(F_{lw}^{-} \sin^2 \frac{\theta}{2} + F_{lw}^{+} \cos^2 \frac{\theta}{2} \right), \tag{27}$$

with $F_{lw}^{\pm} = \sigma \bar{R}_{lw}^{\pm}$. We can observe that $\hat{\rho}_{D,lw}$ is traceless in λ^2 , and that its terms carry the parameters that characterize the gravitational plane wave in the long-wavelength regime, clearly showing the signature of the gravitational wave background in the system. The integral given in (24) has the following result

$$C_{lw}^{\pm} = \frac{\bar{a}\sigma\sqrt{\pi}}{4\pi^2\sqrt{1-\mathcal{A}^2}} e^{-\sigma^2}. \tag{28}$$

With these results, we can investigate how the off-diagonal elements of Eq. (19) behaved as a function of acceleration. Starting from (22) and (23), we can substitute the following expressions (28) and (27), and with some algebraic manipulations we obtain

$$\hat{\rho}_{D,lw}^{eg} = \frac{1}{2} \sin \theta \left\{ e^{-i\chi} + \lambda^2 \left[e^{+i\chi} C_{lw}^{+} - \sigma e^{-i\chi} \left(\bar{R}_{lw}^{-} \sin^2 \frac{\theta}{2} + \bar{R}_{lw}^{+} \cos^2 \frac{\theta}{2} \right) \right] \right\}, \tag{29}$$

$$\hat{\rho}_{D,lw}^{ge} = \frac{1}{2} \sin \theta \left\{ e^{+i\chi} + \lambda^2 \left[e^{-i\chi} C_{lw}^{+} - \sigma e^{+i\chi} \left(\bar{R}_{lw}^{-} \sin^2 \frac{\theta}{2} + \bar{R}_{lw}^{+} \cos^2 \frac{\theta}{2} \right) \right] \right\}, \tag{30}$$

where \bar{R}_{lw}^{-} and \bar{R}_{lw}^{+} are given by (10) and (11). In Fig. 2, we plot the off-diagonal elements (29) and (30), as a function of acceleration considering different values for the phase shifts. As shown by Fig. 2a, b, the off-diagonal elements are degraded as the acceleration increases, additionally, we can observe that this degradation is amplified for values of $\delta_{+/\times} \neq \pi/2$, unlike in the case of $\delta_{+/\times} = \pi/2$ where we obtain the results for Minkowski space. We discuss these degradation effects in more detail in Sect. 5.

In a two-level quantum system, we can obtain the degree of coherence between the two states of this system through something called l^1 norm quantum coherence. This type of coherence captures the phenomena caused by quantum superposition effects between the states of the system. In other words, for the case of our system given by the matrix (19), the corresponding l^1 norm quantum coherence is determined by the sum of the modulus of the off-diagonal elements [16], and then we have

$$C^{l^1}(\hat{\rho}) = \sum_{i \neq j} |\hat{\rho}^{ij}|, \tag{31}$$

and for our setup, considering the large interaction time regime, e.g. $\sigma \gg 1$, we have

$$C_{lw}^{l^1} \approx \sin \theta \left[1 - \frac{1}{2\pi\sqrt{1-\mathcal{A}^2}} \frac{\sigma\lambda^2}{e^{2\pi/\bar{a}} - 1} \left(\sin^2 \frac{\theta}{2} + e^{2\pi/\bar{a}} \cos^2 \frac{\theta}{2} \right) \right] + \mathcal{O}(g^4), \tag{32}$$

thus, finally, we obtain the l^1 norm quantum coherence for a qubit accelerated in a gravitational wave background, in the long-wavelength and large interaction time regime. It is important to note that (32) depends on the parameters that characterize the monochromatic gravitational plane wave, this dependence must generate effects on coherence degradation.

As discussed by [41], is surprising that a detector with no apparent spatial extension can sense the presence of a gravitational wave, as sensing the tidal force requires a certain spatial extension. They also add that one could try to argue

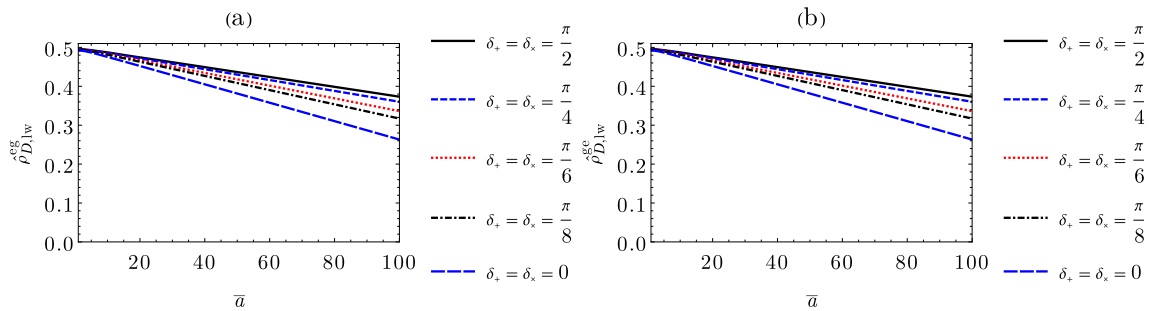


Fig. 2 **a** $\hat{\rho}_{D,lw}^{eg}$ and **b** $\hat{\rho}_{D,lw}^{gc}$ for different phase shifts $\delta_{+/\times}$ as a function of the dimensionless parameter \bar{a} . We leave the following values fixed: $\theta = \pi/2, \lambda = 0.1, \sigma = 10,$ and $A_+ = A_\times = 0.65$

that the Unruh–DeWitt detector has an intrinsic energy scale Ω , and according to the energy-time uncertainty principle, it exhibits a temporal scale of $\sim 1/\Omega$, which in turn gives rise to a spatial scale of $\sim v/\Omega$, where $v < 1$ is the velocity of the detector. However, even if the detector has a finite extent δl , the tidal force produced by a gravitational wave over a spatial separation of δl is proportional to $(\delta l)\ddot{h}_{+/\times} \sim \mathcal{A}_{+/\times}\omega^2\delta l$, which vanishes in the long-wavelength limit ($\omega \rightarrow 0$). Since the correction $1/\sqrt{1-\mathcal{A}^2}$ survives the formal limit $\omega \rightarrow 0$, this gravitational wave effect in a quantum system is qualitatively different from that in a classical mechanical system and cannot be understood in terms of the gravitational-wave tidal force. This is a genuine quantum effect with no classical analogue.

4 Quantum interferometric circuit

In this section we discuss the quantum scattering circuit as shown in Fig. 3. This circuit is structured as follows: Initially, a single qubit is in a well-known initial state. Soon after, the first Hadamard gate modifies the qubit state to a superposition state. Next, a unitary operator \mathcal{U} and a phase change α are applied simultaneously. In this step, the qubit interacts with a massless scalar field in a gravitational wave background in a controlled way. At last, the qubit passes through the second Hadamard gate and then system measurements are carried out.

In this setup, the qubit used in the quantum interferometric circuit is initially described by the density matrix $\hat{\rho}_I^g = |g\rangle\langle g|$, the actuation of the first Hadamard gate gives us the following expression

$$\hat{\rho}_I^{\text{in}} = \frac{1}{2} (|g\rangle\langle g| + |g\rangle\langle e| + |e\rangle\langle g| + |e\rangle\langle e|). \tag{33}$$

The density matrix that represents the field in the vacuum state is $\hat{\rho}_\phi = |0\rangle\langle 0|$, and therefore, the initial representation of the system is given by $\hat{\rho}_{\text{in}} = \hat{\rho}_I^{\text{in}} \otimes \hat{\rho}_\phi$. The probability amplitude of finding the qubit in the state $|g\rangle$ or $|e\rangle$ between the Hadamard gates has a phase accumulation, a phase α

is added by the phase-shift gate if the qubit is in $|e\rangle$. The detector-field interaction happens similarly as shown in the previous setup by the operation of the operator \mathcal{U} in the perturbative form (15). And finally, after the accumulation of quantum phase and detector-field interaction, applying the second Hadamard gate and plotting out the degrees of freedom of the field, we obtain the density matrix that expresses the final configuration of the detector, which reads as

$$\begin{aligned} \hat{\rho}_{I,lw} = & \left\{ \cos^2 \frac{\alpha}{2} + \frac{\lambda^2}{4} [\mathcal{F}_{lw}^- + \mathcal{F}_{lw}^+ \right. \\ & \left. - 8\text{Re}(\mathcal{G}_{lw}^-) \cos^2 \frac{\alpha}{2} + 2\mathcal{C}_{lw}^- \cos \alpha] \right\} |g\rangle\langle g| \\ & + \left\{ \sin^2 \frac{\alpha}{2} + \frac{\lambda^2}{4} [\mathcal{F}_{lw}^- + \mathcal{F}_{lw}^+ \right. \\ & \left. - 8\text{Re}(\mathcal{G}_{lw}^-) \sin^2 \frac{\alpha}{2} - 2\mathcal{C}_{lw}^- \cos \alpha] \right\} |e\rangle\langle e| \\ & + \left\{ -\frac{i}{2} \sin \alpha + \frac{\lambda^2}{4} [\mathcal{F}_{lw}^- - \mathcal{F}_{lw}^+ \right. \\ & \left. + 2i \sin \alpha (2\text{Re}(\mathcal{G}_{lw}^-) - \mathcal{C}_{lw}^-)] \right\} |g\rangle\langle g| \\ & + \left\{ +\frac{i}{2} \sin \alpha + \frac{\lambda^2}{4} [\mathcal{F}_{lw}^- - \mathcal{F}_{lw}^+ \right. \\ & \left. - 2i \sin \alpha (2\text{Re}(\mathcal{G}_{lw}^-) - \mathcal{C}_{lw}^-)] \right\} |g\rangle\langle e|, \end{aligned} \tag{34}$$

where it must obey the following relation to be traceless in λ^2

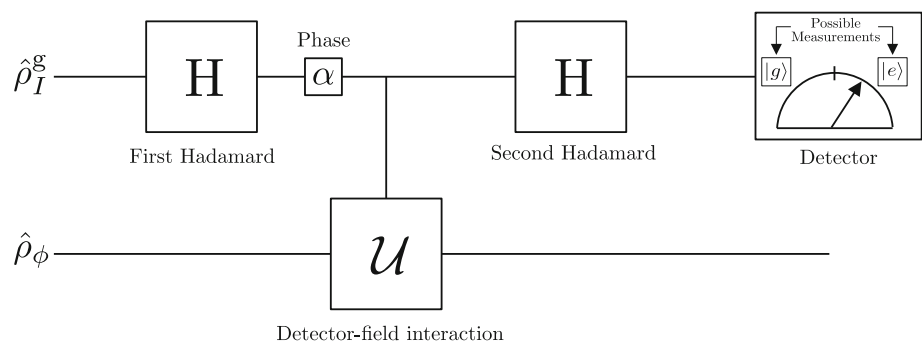
$$\text{Re}(\mathcal{G}_{lw}^-) = \frac{1}{4} (\mathcal{F}_{lw}^- + \mathcal{F}_{lw}^+). \tag{35}$$

Using the reduced density matrix of the detector (34) we can obtain the probability of finding the system in the ground state $P_{I,lw}^g = \langle g|\hat{\rho}_{I,lw}|g\rangle$, using (35) and $\mathcal{F}_{lw}^\pm = \sigma \bar{R}^\pm$ which results as follows

$$P_{I,lw}^g = \cos^2 \frac{\alpha}{2} - \sigma \cos \alpha \frac{\lambda^2}{4} \left(\bar{R}_{lw}^- + \bar{R}_{lw}^+ - \frac{2\mathcal{C}_{lw}^-}{\sigma} \right). \tag{36}$$

Now, we are able to obtain the information about the interference pattern of our quantum interferometric circuit. Interferometric visibility (or just visibility) is a measure of the

Fig. 3 Schematic representation of a quantum interferometric circuit in Unruh effect scenario in a gravitational wave background



interference contrast in any system in superposition situations. It offers a practical way to measure the coherence of two waves (or a wave with itself). Visibility is defined as the ratio between the amplitude of the interference pattern and the sum of the individual powers, mathematically we have

$$V_{I, \text{lw}} = \frac{P_{I, \text{lw}}^{\text{g,max}} - P_{I, \text{lw}}^{\text{g,min}}}{P_{I, \text{lw}}^{\text{g,max}} + P_{I, \text{lw}}^{\text{g,min}}}, \tag{37}$$

where the probability $P_{I, \text{lw}}^{\text{g}}$ has the maximum (minimum) value when $\alpha = 0$ ($\alpha = \pi$), and then, when we assume the large interaction time limit ($\sigma \gg 1$), we get

$$V_{I, \text{lw}} \approx 1 - \frac{\sigma \lambda^2}{4\pi \sqrt{1 - \mathcal{A}^2}} \coth\left(\frac{\pi}{\bar{a}}\right), \tag{38}$$

where this expression is the visibility of the interference pattern under the Unruh effect of the quantum interferometric circuit in a gravitational wave background, in the long-wavelength regime and great interaction time. On the other hand, we can also obtain the l^1 norm quantum coherence of our interferometric setup, using the reduced density matrix (34) and adding the absolute values of its off-diagonal elements, we have the coherence is given by

$$C_{I, \text{lw}}^{l^1} \approx \sin \alpha \left[1 - \frac{\sigma \lambda^2}{4\pi \sqrt{1 - \mathcal{A}^2}} \coth\left(\frac{\pi}{\bar{a}}\right) \right], \tag{39}$$

where we have the relationship $C_{I, \text{lw}}^{l^1} \approx \sin \alpha V_{I, \text{lw}}$.

5 Numerical results

Considering the presence of a background gravitational wave in the long wavelength regime ($\omega \rightarrow 0$) that interacts with the massless scalar field for a large period of time ($\sigma \gg 1$), we performed a numerical analysis of the l^1 norm quantum coherence $C_{\text{lw}}^{l^1}$ of an accelerated single-qubit (Fig. 4a) and the visibility $V_{I, \text{lw}}$ of the quantum interferometric circuit (Fig. 4b), both were plotted as a function of the dimensionless parameter \bar{a} for different phase shifts $\delta_{+/\times}$. We can note that when $\delta_+ = \delta_\times = \pi/2$ we have $\mathcal{A} = 0$, and we obtain the standard result without influence of gravitational wave. On the other hand, when $\delta_+ = \delta_\times = \pi/4, \pi/6, \pi/8$, we can see

that both coherence and visibility gradually decrease to these respective values, and in $\delta_+ = \delta_\times = 0$ reaches its minimum value. Indicating that changes in the detector's internal states are amplified and this, consequently, also amplifies the coherence degradation of an accelerated qubit and the degradation of the interferometer's interference fringes.

Now, considering Fig. 5, we have $C_{\text{lw}}^{l^1}$ (Fig. 5a) and $V_{I, \text{lw}}$ (Fig. 5b), both plotted as a function of $\delta_{+/\times}$. Note that, considering $\delta_{+/\times} = n\pi$, for $n = 0, 1, 2, \dots$, that is, when the phase shifts are integer multiples of π we have that the degradation of coherence and interference fringes reach their maximum, indicating that the polarization modes of the gravitational wave had a totally constructive interference, i.e., acting in resonance, and consequently amplified the system's coherence degradation mechanism. Additionally, for $n = 1/2, 3/2, 5/2, \dots$, that is, when the phase shifts are a semi-integer number of π we have that the polarization modes have a totally destructive interference (are out of phase), and the coherence degradation mechanism is not changed.

As shown in Fig. 6, we plot $C_{\text{lw}}^{l^1}$ (Fig. 6a) and $V_{I, \text{lw}}$ (Fig. 6b) as a function of the amplitudes of the $A_{+/\times}$, and note that coherence degradation and visibility loss increase with increasing amplitudes, provided that the combination of these amplitudes obeys $\mathcal{A}^2 < 1$, due to linearized theory. We can see that the coherence degradation of the system is amplified due to the increase in amplitude since the greater the amplitude, the greater the amount of energy transported.

Thus, as we have seen, the gravitational wave background amplifies the Unruh effect through the transfer of energy from the gravitational wave to the internal states of the detector, this effect also amplifies the coherence degradation and visibility loss in situations of long wavelength, long interaction time, polarization modes in resonance and with small amplitudes.

6 Conclusions

We investigate the effects of a background gravitational wave on the coherence degradation mechanism of two setups. The first is composed of a two-level system initially prepared in a qubit state that is uniformly accelerated and interacts with

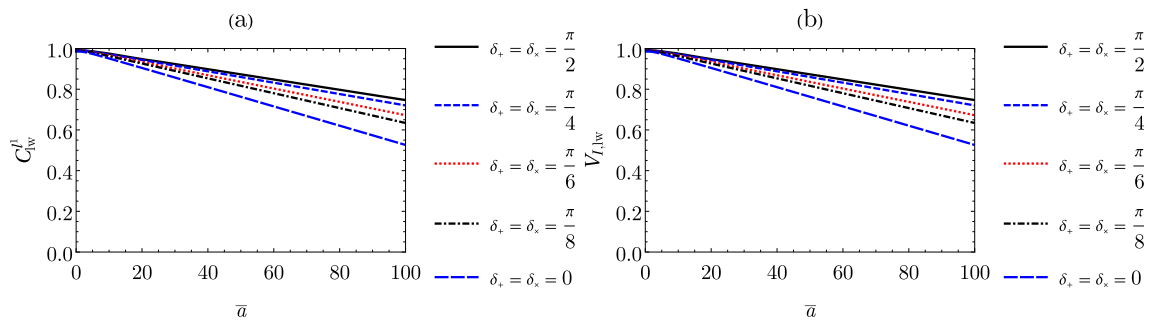


Fig. 4 **a** C_{lw}^I and **b** $V_{I,lw}$ for different phase shifts $\delta_{+/\times}$ as a function of the dimensionless parameter \bar{a} . We leave the following values fixed: $\theta = \pi/2, \lambda = 0.1, \sigma = 10,$ and $A_+ = A_\times = 0.65$

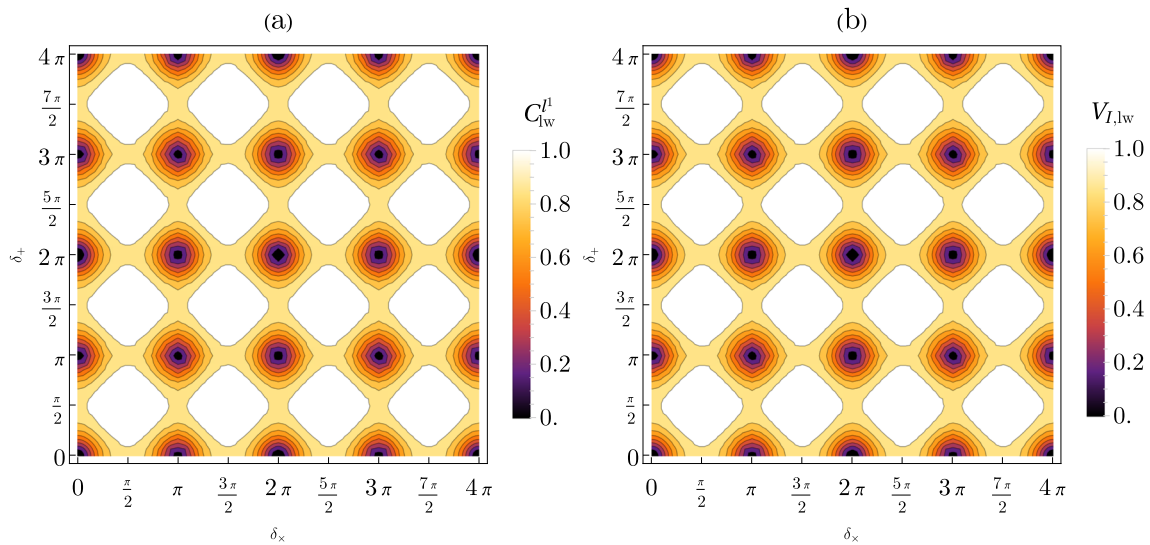


Fig. 5 **a** C_{lw}^I and **b** $V_{I,lw}$ as a function of the phase shifts $\delta_{+/\times}$, with the following values fixed: $\theta = \pi/2, \lambda = 0.1, \bar{a} = 100, \sigma = 10,$ and $A_+ = A_\times = 0.65$

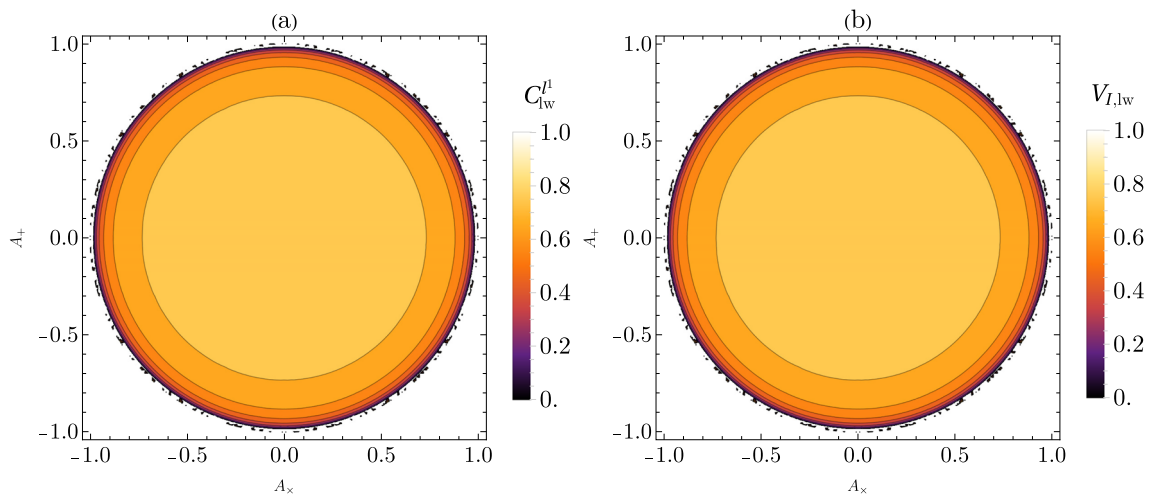


Fig. 6 **a** C_{lw}^I and **b** $V_{I,lw}$ as a function of the amplitudes of polarization modes $A_{+/\times}$. We consider the following fixed values: $\theta = \pi/2, \lambda = 0.1, \bar{a} = 100, \sigma = 10,$ and $\delta_{+/\times} = 0$

a massless scalar field for a finite time. The second is a quantum interferometric circuit neatly composed of a Hadamard gate, phase change gate and interaction detector-field during a finite time, Hadamard gate and measurement of the internal states of the detector. In first setup, we calculate the probability transition rates and the l^1 norm quantum coherence, in second setup we calculate the visibility, in the gravitational wave background in the long-wavelength regime ($\omega \rightarrow 0$) and large interaction time ($\sigma \gg 1$).

Therefore, our findings indicate that the gravitational wave background plays an amplifier role for the coherence degradation mechanism. This occurs through the transfer of energy from the gravitational wave to the internal states of the detector, causing, together with the Unruh effect, variations in these internal states. This amplification occurs when polarization modes are in resonance, this effect is proportional to the amplitudes and phase shifts in the regime in which amplitudes must be modulated to be small ($\mathcal{A}^2 < 1$) as imposed by linearized theory.

It was also possible to note that for the case of short-wavelength ($\omega \rightarrow \infty$) of the gravitational wave, the transition rate probability, and consequently the coherence degradation and visibility, are equal to the standard result without a gravitational wave. The reason the Unruh–DeWitt detector does not respond to the gravitational wave in this limit is because the wave oscillation is so fast that the detector does not have time to respond to this oscillation within the timescale $\approx 1/\Omega$ for the two-level transition.

Concerning the practical aspect of the possible experimental application of our model, we emphasize that our investigation here is mainly for theoretical concerns. Experimentally, measuring the response of the Unruh–DeWitt detector is extremely challenging, probably beyond the reach of current technology. Our results indicate that the gravitational wave response seems to be measurable for large enough amplitudes. However, since the transition rate in principle has to be measured by a large array of identical detectors [47] the interactions between the detectors in the array and between the system and its surroundings will introduce noise that will spoil the signal in response to a gravitational wave that is extremely weak upon arrival at Earth.

Acknowledgements PHMB acknowledges the Brazilian funding agency CAPES for financial support.

Data Availability Statement This manuscript has no associated data. [Authors' comment: Data sharing does not apply as no datasets were generated or analyzed during the current study.]

Code Availability Statement This manuscript has no associated code/software. [Authors' comment: Code/software sharing does not apply as no code/software was generated or analyzed during the current study.]

Declarations

Conflict of interest Not applicable.

Open Access This article is licensed under a Creative Commons Attribution 4.0 International License, which permits use, sharing, adaptation, distribution and reproduction in any medium or format, as long as you give appropriate credit to the original author(s) and the source, provide a link to the Creative Commons licence, and indicate if changes were made. The images or other third party material in this article are included in the article's Creative Commons licence, unless indicated otherwise in a credit line to the material. If material is not included in the article's Creative Commons licence and your intended use is not permitted by statutory regulation or exceeds the permitted use, you will need to obtain permission directly from the copyright holder. To view a copy of this licence, visit <http://creativecommons.org/licenses/by/4.0/>.

Funded by SCOAP³.

A Scalar field and quantization

Here we address the solution of the equation of motion associated with a real scalar field, specifically the Klein-Gordon equation, in a background gravitational wave context. It is noteworthy that space-time is considered flat in the absence of gravitational waves. It is assumed that gravitational waves have a sufficiently weak intensity such that the linearized theory is appropriate. In the linearized formulation, it is possible to decompose any arbitrarily complex gravitational wave into a linear combination of plane waves. In this study, for simplification reasons, we restricted our analysis to a single monochromatic plane wave and also adopted the transverse-trace (TT) gauge. With this in mind, to achieve the objectives of this section we first have to understand the behavior of a scalar field $\phi(x)$ in a curved space-time, so the Lagrangian density that describes this system is given by [48]

$$\mathcal{L} = \frac{1}{2} \sqrt{-g} \left(-g^{\mu\nu} \nabla_\mu \phi \nabla_\nu \phi - m^2 \phi^2 - \xi R \phi^2 \right), \quad (40)$$

where we have that m is the mass, R is the well-known Ricci scalar, and ξ is the coupling constant. Considering now, the simplest case in which our system reduces to the case in which $m = 0$ and $\xi = 0$, which is the well-known equation of motion for the massless scalar field, and thus we obtain

$$\square \phi = 0, \quad (41)$$

where $\square \phi := g^{\mu\nu} \nabla_\mu \nabla_\nu \phi$. Now, we must understand the effects of gravitational waves on scalar fields, so a convenient representation for a gravitational plane wave background is,

$$g_{\alpha\beta}(x) = \eta_{\alpha\beta} + h_{\alpha\beta}(x), \tag{42}$$

$$h_{\alpha\beta}(x) = A_{\alpha\beta} e^{-ik_{\mu}x^{\mu}}, \tag{43}$$

where $h_{\alpha\beta}(x)$ is a perturbation of the metric tensor $g_{\alpha\beta}(x)$ around the flat Minkowski space characterized by $\eta_{\alpha\beta} = \text{diag}(-1, 1, 1, 1)$. Now considering a gravitational plane wave propagating in the z direction, in the TT gauge, we have that the term $h_{\mu\nu}$ becomes [49]

$$h_{\mu\nu}(x) = \begin{pmatrix} 0 & 0 & 0 & 0 \\ 0 & h_{+} & h_{\times} & 0 \\ 0 & h_{\times} & -h_{+} & 0 \\ 0 & 0 & 0 & 0 \end{pmatrix} \tag{44}$$

with

$$h_{+/\times}(x) = A_{+/\times} \cos(kz - \omega t + \delta_{+/\times}), \tag{45}$$

here we have that $\omega = |k|$, h_{+} and h_{\times} are the two independent modes of polarization of the gravitational plane wave with their respective amplitudes A_{+} and A_{\times} and phase shifts δ_{+} and δ_{\times} .

We know that equal-time quantization in curved spacetime needs a time-like Killing vector field to make the idea of time possible, as the metric used here (44) has no similar Killing vector field time, then common quantization method cannot be used. An alternative to solving this problem is to use the light-front quantization formalism [50], in this formalism the direction of time is treated as the direction of the light front based on the light-like Killing vector. The light-front quantization method requires the following switching relations

$$[\phi(\mathbf{x}, u, v), \pi(\mathbf{x}', u', v)] = \frac{i}{2} \sqrt{-g} \delta^2(\mathbf{x} - \mathbf{x}') \delta(u - u'), \tag{46}$$

$$[\pi(\mathbf{x}, u, v), \pi(\mathbf{x}', u', v)] = 0, \tag{47}$$

with $u = (t - z)/\sqrt{2}$ and $v = (t + z)/\sqrt{2}$ being the light-front variables. We can write the mode expansion $\phi(x) \equiv \phi(u, v, \mathbf{x})$ as

$$\phi(x) = \int \frac{d^3k}{(2\pi)^{3/2}} \frac{1}{\sqrt{2k_u}} \left[a_{k_u, \mathbf{k}} f_{k_u, \mathbf{k}}(\mathbf{x}, u, v) + a_{k_u, \mathbf{k}}^{\dagger} f_{k_u, \mathbf{k}}^*(\mathbf{x}, u, v) \right], \tag{48}$$

where $f_{k_u, \mathbf{k}}(\mathbf{x}, u, v) = \exp[i(\mathbf{k} \cdot \mathbf{x} - k_u u - \omega_{k_u, \mathbf{k}} v)] \chi(u)$, with $a_{k_u, \mathbf{k}}^{\dagger}$ and $a_{k_u, \mathbf{k}}$ are the creation and destruction operators, respectively. The commutation relations for the creation and destruction operators are given by

$$[a_{k_u, \mathbf{k}}, a_{k'_u, \mathbf{k}'}^{\dagger}] = \delta^2(\mathbf{k} - \mathbf{k}') \delta(k_u - k'_u), \tag{49}$$

$$[a_{k_u, \mathbf{k}}, a_{k'_u, \mathbf{k}'}] = [a_{k_u, \mathbf{k}}^{\dagger}, a_{k'_u, \mathbf{k}'}^{\dagger}] = 0. \tag{50}$$

We can verify in (48) that the state without particles $|0\rangle$ is the vacuum, and thus we have

$$a_{k_u, \mathbf{k}}|0\rangle = 0, \quad \text{for all } (k_u, \mathbf{k}). \tag{51}$$

Now notice that with these results we can obtain the Wightman function.

References

1. S.A. Fulling, Nonuniqueness of canonical field quantization in Riemannian space-time. *Phys. Rev. D* **7**, 2850–2862 (1973). <https://doi.org/10.1103/PhysRevD.7.2850>
2. P.C.W. Davies, Scalar production in Schwarzschild and Rindler metrics. *J. Phys. A Math. Gen.* **8**(4), 609 (1975). <https://doi.org/10.1088/0305-4470/8/4/022>
3. W.G. Unruh, Notes on black-hole evaporation. *Phys. Rev. D* **14**, 870–892 (1976). <https://doi.org/10.1103/PhysRevD.14.870>
4. B.S. DeWitt, *Quantum Gravity: The New Synthesis* (Cambridge University Press, 1980), pp. 680–745. <https://ui.adsabs.harvard.edu/abs/2010grae.book.....H>
5. R.B. Mann, T.C. Ralph, Relativistic quantum information. *Class. Quantum Gravity* **29**(22), 220301 (2012). <https://doi.org/10.1088/0264-9381/29/22/220301>
6. S.W. Hawking, Particle creation by black holes. *Commun. Math. Phys.* **43**(3), 199–220 (1975)
7. R.M. Wald, *Quantum Field Theory in Curved Spacetime and Black Hole Thermodynamics* (University of Chicago Press, Chicago, 1994)
8. E. Adlam, A. Kent, Device-independent relativistic quantum bit commitment. *Phys. Rev. A* **92**, 022315 (2015). <https://doi.org/10.1103/PhysRevA.92.022315>
9. A.G.S. Landulfo, Nonperturbative approach to relativistic quantum communication channels. *Phys. Rev. D* **93**, 104019 (2016). <https://doi.org/10.1103/PhysRevD.93.104019>
10. A. Pozas-Kerstjens, E. Martín-Martínez, Harvesting correlations from the quantum vacuum. *Phys. Rev. D* **92**, 064042 (2015). <https://doi.org/10.1103/PhysRevD.92.064042>
11. A. Pozas-Kerstjens, E. Martín-Martínez, Entanglement harvesting from the electromagnetic vacuum with hydrogenlike atoms. *Phys. Rev. D* **94**, 064074 (2016). <https://doi.org/10.1103/PhysRevD.94.064074>
12. P. Simidzija, A. Ahmadzadegan, A. Kempf, E. Martín-Martínez, Transmission of quantum information through quantum fields. *Phys. Rev. D* **101**, 036014 (2020). <https://doi.org/10.1103/PhysRevD.101.036014>
13. E. Tjoa, E. Martín-Martínez, When entanglement harvesting is not really harvesting. *Phys. Rev. D* **104**, 125005 (2021). <https://doi.org/10.1103/PhysRevD.104.125005>
14. E. Tjoa, Quantum teleportation with relativistic communication from first principles. *Phys. Rev. A* **106**, 032432 (2022). <https://doi.org/10.1103/PhysRevA.106.032432>
15. A. Laponi, D. Moustos, D.E. Bruschi, S. Mancini, Relativistic quantum communication between harmonic oscillator detectors. *Phys. Rev. D* **107**, 125010 (2023). <https://doi.org/10.1103/PhysRevD.107.125010>
16. T. Baumgratz, M. Cramer, M.B. Plenio, Quantifying coherence. *Phys. Rev. Lett.* **113**, 140401 (2014). <https://doi.org/10.1103/PhysRevLett.113.140401>

17. J. Wang, Z. Tian, J. Jing, H. Fan, Irreversible degradation of quantum coherence under relativistic motion. *Phys. Rev. A* **93**, 062105 (2016). <https://doi.org/10.1103/PhysRevA.93.062105>
18. Z. Huang, H. Situ, Quantum coherence behaviors of fermionic system in non-inertial frame. *Quantum Inf. Process.* **17**(4), 1–18 (2018). <https://doi.org/10.1007/s11128-018-1867-0>
19. Z. Huang, W. Zhang, Quantum coherence behaviors for a uniformly accelerated atom immersed in fluctuating vacuum electromagnetic field with a boundary. *Braz. J. Phys.* **49**(2), 161–167 (2019). <https://doi.org/10.1007/s13538-019-00641-0>
20. A.I. Nesterov, M.A. Rodríguez Fernández, G.P. Berman, X. Wang, Decoherence as a detector of the Unruh effect. *Phys. Rev. Res.* **2**, 043230 (2020). <https://doi.org/10.1103/PhysRevResearch.2.043230>
21. W. Zhang, X. Liu, Quantum coherence of a circularly accelerated atom in a spacetime with a reflecting boundary. *Sci. Rep.* **12**(12577), 2045–2322 (2022). <https://doi.org/10.1038/s41598-022-16647-9>
22. Z. Huang, Coherence behaviors of an atom immersing in a massive scalar field. *Eur. Phys. J. D* **76**(4), 67 (2022)
23. S. Harikrishnan, S. Jambulingam, P.P. Rohde, C. Radhakrishnan, Accessible and inaccessible quantum coherence in relativistic quantum systems. *Phys. Rev. A* **105**, 052403 (2022). <https://doi.org/10.1103/PhysRevA.105.052403>
24. P.H.M. Barros, I.G. Paz, O.P.D.S. Neto, H.A.S. Costa, Robustness of wave-particle duality under Unruh effect. *Entropy* (2024). <https://doi.org/10.3390/e26010001>
25. P. H. M. Barros, H. A. S. Costa, Dispersive vacuum as a decoherence amplifier of an Unruh–DeWitt detector. *Journal of Physics A: Mathematical and Theoretical*, **57**(44), 445305 (2024). <https://iopscience.iop.org/article/10.1088/1751-8121/ad860b>
26. F. Benatti, R. Floreanini, Entanglement generation in uniformly accelerating atoms: reexamination of the Unruh effect. *Phys. Rev. A* **70**, 012112 (2004). <https://doi.org/10.1103/PhysRevA.70.012112>
27. H.A.S. Costa, I.G. da Paz, P.R.S. Carvalho, M. Sampaio, Ramsey interferometry as a witness of acceleration radiation. *Ann. Phys.* **416**, 168158 (2020). <https://doi.org/10.1016/j.aop.2020.168158>
28. C. Gooding, S. Biermann, S. Erne, J. Louko, W.G. Unruh, J. Schmiedmayer, S. Weinfurter, Interferometric Unruh detectors for Bose–Einstein condensates. *Phys. Rev. Lett.* **125**(21), 213603 (2020)
29. H.T. Lopes, I.G. da Paz, P.R.S. Carvalho, H.A.S. Costa, Thermal signature of the Unruh effect in the interference pattern. *Phys. Lett. A* **409**, 127483 (2021). <https://doi.org/10.1016/j.physleta.2021.127483>
30. A.M. Souza, I.S. Oliveira, R.S. Sarthour, A scattering quantum circuit for measuring bell’s time inequality: a nuclear magnetic resonance demonstration using maximally mixed states. *New J. Phys.* **13**(5), 053023 (2011). <https://doi.org/10.1088/1367-2630/13/5/053023>
31. C. Negrevergne, R. Somma, G. Ortiz, E. Knill, R. Laflamme, Liquid-state NMR simulations of quantum many-body problems. *Phys. Rev. A* **71**, 032344 (2005). <https://doi.org/10.1103/PhysRevA.71.032344>
32. U. Leonhardt, Quantum-state tomography and discrete Wigner function. *Phys. Rev. Lett.* **74**, 4101–4105 (1995). <https://doi.org/10.1103/PhysRevLett.74.4101>
33. J. Garriga, E. Verdaguer, Scattering of quantum particles by gravitational plane waves. *Phys. Rev. D* **43**, 391–401 (1991). <https://doi.org/10.1103/PhysRevD.43.391>
34. P.-M. Zhang, C. Duval, G.W. Gibbons, P.A. Horvathy, The memory effect for plane gravitational waves. *Phys. Lett. B* **772**, 743–746 (2017). <https://doi.org/10.1016/j.physletb.2017.07.050>
35. P.-M. Zhang, C. Duval, G.W. Gibbons, P.A. Horvathy, Velocity memory effect for polarized gravitational waves. *J. Cosmol. Astropart. Phys.* **2018**(05), 030 (2018). <https://doi.org/10.1088/1475-7516/2018/05/030>
36. P. Jones, P. McDougall, D. Singleton, Particle production in a gravitational wave background. *Phys. Rev. D* **95**, 065010 (2017). <https://doi.org/10.1103/PhysRevD.95.065010>
37. P. Jones, P. McDougall, M. Ragsdale, D. Singleton, Scalar field vacuum expectation value induced by gravitational wave background. *Phys. Lett. B* **781**, 621–625 (2018). <https://doi.org/10.1016/j.physletb.2018.04.055>
38. S. Morales, A. Dasgupta, Scalar and fermion field interactions with a gravitational wave. *Class. Quantum Gravity* **37**(10), 105001 (2020). <https://doi.org/10.1088/1361-6382/ab79d6>
39. Q. Xu, S. Ali Ahmad, A.R.H. Smith, Gravitational waves affect vacuum entanglement. *Phys. Rev. D* **102**, 065019 (2020). <https://doi.org/10.1103/PhysRevD.102.065019>
40. R. Haasteren, T. Prokopec, Scalar propagator for planar gravitational waves. *arXiv preprint arXiv:2204.12930* (2022)
41. B.-H. Chen, D.-W. Chiou, Response of the Unruh–Dewitt detector in a gravitational wave background. *Phys. Rev. D* **105**, 024053 (2022). <https://doi.org/10.1103/PhysRevD.105.024053>
42. T. Prokopec, Gravitational wave signals in an Unruh–Dewitt detector. *Class. Quantum Gravity* **40**(3), 035007 (2023). <https://doi.org/10.1088/1361-6382/acabf5>
43. Y. Sugiyama, K. Yamamoto, T. Kobayashi, Gravitational waves in Kasner spacetimes and Rindler wedges in Regge–Wheeler gauge: formulation of Unruh effect. *Phys. Rev. D* **103**(8), 083503 (2021)
44. T. Padmanabhan, General covariance, accelerated frames and the particle concept. *Astrophys. Space Sci.* **83**, 247–268 (1982)
45. J.R. Letaw, J.D. Pfautsch, Quantized scalar field in the stationary coordinate systems of flat spacetime. *Phys. Rev. D* **24**(6), 1491 (1981)
46. L. Sriramkumar, T. Padmanabhan, Finite-time response of inertial and uniformly accelerated Unruh–Dewitt detectors. *Class. Quantum Gravity* **13**(8), 2061 (1996)
47. D.-W. Chiou, Response of the Unruh–Dewitt detector in flat spacetime with a compact dimension. *Phys. Rev. D* **97**, 124028 (2018). <https://doi.org/10.1103/PhysRevD.97.124028>
48. N.D. Birrell, P.C.W. Davies, *Quantum Fields in Curved Space* (Cambridge University Press, 1984). <https://books.google.com/books?id=SEnaUnrqzrUC>
49. S.M. Carroll, *Spacetime and Geometry* (Cambridge University Press, Cambridge, 2019)
50. M. Burkardt, in *Light Front Quantization*, ed. by J.W. Negele, E. Vogt (Springer, Boston, 2002), pp.1–74. https://doi.org/10.1007/0-306-47067-5_1